doi:10.1093/brain/awm155 *Brain* (2007), **130**, 2159–2174

Grafts of Schwann cells engineered to express PSA-NCAM promote functional recovery after spinal cord injury

Florentia Papastefanaki,[1,*] Jian Chen,[2,*] Alexandros A. Lavdas,[1] Dimitra Thomaidou,[1] Melitta Schachner[2] and Rebecca Matsas[1]

[1]Laboratory of Cellular and Molecular Neurobiology, Hellenic Pasteur Institute, 127 Vas. Sofias Ave, 11521 Athens, Greece and [2]W.M. Keck Center for Collaborative Neuroscience, Rutgers University, 604 Allison Road, Piscataway, NJ 08854-8082, USA

*These authors contributed equally to this work.

Correspondence to: Rebecca Matsas, Laboratory of Cellular and Molecular Neurobiology, Hellenic Pasteur Institute, 127 Vassilissis Sofias, 11521 Athens, Greece
E-mail: rmatsa@pasteur.gr

Schwann cells (SCs) are among the most attractive cellular candidates for the development of remyelination therapies for CNS lesions. Yet, their integration in the CNS is inhibited by astrocytes and therefore the use of genetically modified SCs with improved properties is an alternative promising approach. Our strategy for ameliorating the therapeutic potential of SCs has been to alter their adhesive properties by expressing on their surface the polysialylated (PSA) form of the neural cell adhesion molecule NCAM. In the present study, SCs from transgenic GFP-mice were transduced with a retroviral vector encoding sialyl-transferase X (STX), the enzyme responsible for transferring PSA on NCAM. Engineered STX-GFP-SCs with sustained PSA expression were thus generated and were found to have improved ability to associate with astrocytes *in vitro*. Importantly, when these cells were transplanted *in vivo* in a mouse model of spinal cord injury they promoted faster and significantly greater functional recovery as compared to using SCs transduced with a control retroviral vector or no cells at all. Morphological analysis indicated that the improved locomotor recovery correlated with earlier and enhanced remyelination by grafted STX-GFP-SCs, increased remyelination by host SCs as well as enhanced differentiation/remyelination by resident oligodendrocyte precursors. Moreover, sprouting of regenerating serotonergic nerve fibres, which are known to be important for locomotion and recovery after injury, was observed into and across the lesion site. These results underline the potential therapeutic benefit of early activation of myelin-forming cells to differentiate and remyelinate severed axons thus restoring functions in CNS trauma and/or demyelinating diseases.

Keywords: CNS; gene therapy; regeneration; remyelination; retroviral gene transfer

Abbreviations: AP = alkaline phosphatase; GFP = green fluorescent protein; SC = Schwann cell; SCI = spinal cord injury; STX = sialyl-transferase X

Received January 11, 2007. Revised June 1, 2007. Accepted June 13, 2007. Advance Access publication July 11, 2007

Introduction

Demyelination occurs in several CNS disorders, including multiple sclerosis, viral infection and spinal cord injury (SCI) and can result in severe functional impairment. Therefore there is great interest in developing therapies promoting repair in CNS demyelinating diseases and trauma (Halfpenny *et al.*, 2002; Thuret *et al.*, 2006). Cell replacement therapy is an attractive approach for myelin repair (Bunge and Pearse, 2003; Pearse and Bunge, 2006) and experimental transplantation has provided overwhelming evidence of the repair potential of grafted myelin-forming cells. Schwann cells (SCs), oligodendrocytes, olfactory ensheathing cells and, more recently, embryonic and neural stem cells have been shown to form myelin after transplantation into the demyelinated CNS (Brustle *et al.*, 1999; Blakemore and Franklin, 2000; Zhang and Duncan, 2000; Pearse *et al.*, 2004; Fouad *et al.*, 2005; Pluchino and Martino, 2005). So far, each cell type has its own advantages and limitations. However, SCs are among the most promising candidates for autologous grafting. They can remyelinate spinal cord lesions after experimental demyelination leading in some cases to

functional recovery in both rodent and primate demyelination models (Honmou *et al.*, 1996; Baron-Van Evercooren *et al.*, 1997; Franklin, 2002; Takami *et al.*, 2002; Pearse *et al.*, 2004; Bachelin *et al.*, 2005; Fouad *et al.*, 2005; Girard *et al.*, 2005). Importantly, the development of *in vitro* systems to harvest and expand human SCs presents a unique opportunity for autologous transplantation in the clinic (Levi *et al.*, 1995; Rutkowski *et al.*, 1995). However, one major issue that still needs to be addressed is the poor integration of SCs within the CNS primarily caused by their limited motility in the CNS environment. SCs do not normally enter the CNS (Blakemore and Franklin, 2000) and migration of SCs transplanted in rodent CNS white matter is inhibited by astrocytes (Blakemore and Franklin, 2000; Iwashita *et al.*, 2000). Overcoming this obvious disadvantage is critical before SCs can be used for efficacious therapeutic intervention.

Our strategy for improving the therapeutic potential of SCs has been to alter their adhesive properties. The neural cell adhesion molecule NCAM is expressed on axonal and SC membranes (Storms and Rutishauser, 1998) and its properties are influenced by polysialylation, a mediator of neural cell migration and axon pathfinding (Kiss and Rougon, 1997; Muller *et al.*, 2000). Polysialic acid (PSA) is synthesized on NCAM by polysialyltransferase (PST) and sialyl-transferase X (STX) (Angata and Fukuda, 2003). Expression of PSA on NCAM is up-regulated during CNS development and down-regulated postnatally while it persists in the adult brain only in areas of neuronal remodeling and plasticity (Durbec and Cremer, 2001). PSA is also associated with oligodendrocyte precursor migration during development and regeneration. Notably, PSA is expressed by oligodendrocyte precursors, reactive astrocytes and SCs for the first 2 weeks after spinal cord demyelination, suggesting a role for PSA in glial plasticity and axonal growth after injury (Oumesmar *et al.*, 1995). Nevertheless, embryonic and perinatal SCs do not express PSA although they do express NCAM (Thomaidou *et al.*, 2001; Lavdas *et al.*, 2006). We therefore reasoned that PSA expression on NCAM present on the SC surface would be beneficial for their better integration in the injured CNS.

To test this hypothesis we have recently generated genetically engineered SCs with sustained PSA expression via transduction with a retroviral vector encoding STX (STX-SCs) (Lavdas *et al.*, 2006). STX-SCs exhibited enhanced migratory potential *in vitro* both in dissociated cell cultures and when grafted in brain slice cultures, without impairment of their myelinating ability (Lavdas *et al.*, 2006). As PSA down-regulation is a prerequisite for myelination to occur (Charles *et al.*, 2000), a critical property of the STX-SCs was that PSA was readily down-regulated when these cells were either primed for or actively engaged in myelination *in vitro*. Importantly, when used *in vivo* STX-SCs enhanced the repair process in a rat model of peripheral nerve injury (Gravvanis *et al.*, 2005). These observations prompted us to test whether transplantation of STX-SCs is of therapeutic value in a mouse model of SCI. Here we demonstrate that grafts of STX-SCs result in improved repair, both morphologically and functionally, as compared to using SCs transduced with a control retroviral vector or no cells at all. Our results suggest that STX-SCs have significant therapeutic potential for the treatment of SCI.

Materials and Methods

Schwann cell-culture preparation, transduction and selection

Schwann cells (GFP-SCs) from postnatal day (P) 5 transgenic C57BL/6J mice, expressing the green fluorescent protein (GFP) under the control of beta-actin promoter (Jackson Laboratories), were prepared and purified from sciatic nerves as previously described (Meintanis *et al.*, 2001). SC purity was >95% as estimated by immunostaining for the SC markers glial fibrillary acidic protein (GFAP) and S100 protein. SC expansion with forskolin (2 μM, Sigma, St Louis, MO, USA) and β-heregulin (HRG-β, 250 ng/ml, R&D Systems, Minneapolis, MN, USA) followed by transduction with pREV retrovirus encoding either for STX or the control protein alkaline phosphatase (AP), were performed as in (Lavdas *et al.*, 2006). For selection, cells were exposed to 200 μg/ml G418 (Gibco BRL) in the presence of HRG-β and forskolin for 10 days. Prior to transplantation SCs were centrifuged and resuspended in DMEM at a density of 10^5 cells/μl.

Schwann cell—astrocyte confrontation culture

Astrocytes were purified from neonatal P0-P1 mouse cortices and plated in DMEM/10% FCS in poly-L-lysine-coated tissue culture flasks as described (McCarthy and de Vellis, 1980). When confluent, cells were shaken over 20 h at 120 rpm to remove microglia and oligodendrocyte progenitor cells, resulting in >95% astrocyte purity as determined by GFAP immunostaining. SC-astrocyte confrontation cultures were prepared as described (Lakatos *et al.*, 2000) with slight modifications. Briefly, 10 μl strips containing 10^4 astrocytes or 5×10^4 GFP-SCs transduced for either AP or STX (AP-GFP-SCs or STX-GFP-SCs), were plated parallel to each other on poly-L-lysine coated coverslips (Fig. 2A). Cells were allowed to attach for 1 h before washing with DMEM/10% FCS to remove non-attached cells. Cultures were maintained in DMEM/10% FCS for 3 weeks and were then fixed. The total numbers of GFP-SCs found within the astrocyte domain were counted in 4 coverslips per condition. Statistical analysis was performed using the Student's *t*-test with $P < 0.01$ for significance.

Compression lesion of mouse spinal cord and SC transplantation

All experiments were carried out according to EU regulations and ethical policies. Surgical procedures were performed as described previously (Chen *et al.*, 2005) with slight modifications. Female C57/BL/6J mice, 3 months old, were deeply anaesthetized intraperitoneally with Ketanest (20 vol%, Parke-Davis, Berlin, Germany) and Rompun (8 vol%, Bayer vital, Leverkusen, Germany), 0.01 ml/g body weight. Laminectomy was performed at the T7-T9 level with mouse laminectomy forceps (Fine Science Tools, Heidelberg, Germany). Complete compression injury of

mouse spinal cord was achieved with a pair of watch-maker forceps for 1 s. Injuries were performed by a single operator and, in an initial study, variation of the lesion size was estimated by reconstruction of consecutive parasagittal sections stained for GFAP to demarcate the lesion boundaries (Fig. 4). The lesion volume was consistent, calculated at $0.815 \pm 0.073\,mm^3$.

Immediately after compression lesion 1 µl (10^5 cells) of STX-GFP-SCs, AP-GFP-SCs or DMEM was injected 0.5 mm rostrally to the lesion site using a glass micropipette (tip diameter 100 µm) placed 1 mm deep into the spinal cord. The glass pipette was manipulated with a Nanoliter microinjector (A203XVY, World Precision Instruments, Sarasota, FL) to achieve gentle injection over 5 min. The pipette was then held in place for an extra 2 min, being withdrawn slowly after, and the skin was sutured. After operation, mice were held on a heated cushion before being returned to their home cages. Lesioned animals received 5-bromo-2′-deoxyuridine (BrdU, 1 mg/ml, Sigma) in their drinking water during their survival time. Mice were sacrificed 2 or 4 weeks after operation. Each group of mice grafted with STX-GFP-SCs (STX group) or AP-GFP-SCs (AP group) consisted of two series of six animals (six animals per time point). The group that received DMEM without cells (ungrafted group) consisted of two series of three animals (three animals per time point). Another series of animals (consisting of three animals per group and time point) was sacrificed 1 day, 3 days, 1 and 2 weeks after lesion to closely examine the dynamics of PSA expression.

Immunocytochemistry and immunohistochemistry

PSA expression by STX-GFP-SCs was verified at the end of the selection period and just before transplantation by immunostaining (Lavdas *et al.*, 2006) with mouse monoclonal anti-PSA (1:1000, gift from Dr G. Rougon). Lesioned mice were sacrificed with an overdose of isoflurane (Forenium, ABBOTT) and perfused intracardially with 4% paraformaldehyde in PBS. Spinal cords were dissected into the same fixative overnight at 4°C, cryopreserved and embedded in Tissue-Tek (O.C.T. Compound, BDH). Spinal cord parasagittal cryosections (20 µm) were cut and processed for immunohistochemistry (Chen *et al.*, 2005). Incubation with primary antibodies was overnight at 4°C. For BrdU detection, sections were treated with 2 N HCl/0.1% Triton X-100 for 10 min followed by 0.1 M Sodium Borate, pH 8.5 at room temperature, prior to application of rat anti-BrdU (1:25, Harlan Sera-lab, Loughborough, UK). For detection of peripheral myelin sections were pre-treated for 5 min with ice-cold methanol followed by goat polyclonal anti-P0 (1:100, SantaCruz Biotechnology, Santa Cruz, CA, USA). CNS myelin was identified by rabbit polyclonal anti-proteolipid protein (PLP, 1:200, Abcam, Cambridge, UK). Rabbit polyclonal anti-NG2 chondroitin sulphate proteoglycan (NG2, 1:250, Chemicon, Temecula, CA) was used for the detection of oligodendrocyte precursors. Rabbit polyclonal anti-fibronectin (FN, 1:100, Sigma) and mouse monoclonal anti-GFAP (1:500, Sigma) were used to identify the lesion site and astrogliosis, respectively. Rabbit polyclonal anti-neurofilament 200 (NF-200, 1:500, Sigma) was used to detect neuronal axons while rat monoclonal anti-serotonin (5-HT, 1:50, Chemicon) to identify serotonergic (5-hydroxytryptamine positive, 5-HT$^+$) fibres. Rabbit polyclonal anti-GFP (1:100, Molecular Probes, Eugene, OR, USA) was used in some cases to visualize grafted SCs, even though in most cases they could be observed directly by GFP fluorescence without antibody use. Following primary antibodies, sections were incubated for 2 h with the appropriate secondary antibodies conjugated with AlexaFluor 488 (green), 546 (red) or 647 (blue). Cell nuclei were labelled with TO-PRO-3 (1:1000, Molecular Probes). Specimens were viewed under a Leica TCS SP confocal microscope equipped with 3D analysis software. Expression of AP was assessed by Nitroblue tetrazolium/5-Bromo-4-Chloro-3-Indolyl Phosphate (NBT/BCIP, Sigma) histochemistry (Lavdas *et al.*, 2006) using a Zeiss Axiophot photomicroscope equipped with a Leica DC-300 digital camera.

Behavioural assay

Hind limb locomotor function was assessed using the Basso Mouse Scale (BMS) (Engesser-Cesar *et al.*, 2005). Locomotor performance of each animal was evaluated during free movement in an open field arena placed 90 cm over ground to aid close observations of the mice. All lesioned animals were tested and recorded by a video camera for 4 min, weekly after operation. BMS score was 0 (flaccid paralysis) for all lesioned animals 1 day after operation. Scoring was done in a double-blind manner by an independent observer. Statistical analysis was performed using one way ANOVA with $P < 0.05$ for significance.

Quantification and statistical analysis

Estimation of remyelination by SCs was done by counting all P0 positive internodes surrounding NF-200-labelled axons in the total area of seven sections spaced 80 µm apart for each animal, scanned at 40× ($n = 6$/series for STX and AP groups and $n = 3$/series for the ungrafted group). Because it is difficult to distinguish individual CNS internodes, estimation of remyelination of CNS origin was done by image processing using the Image-Pro Plus image analysis software. Confocal images of PLP immunofluorescence staining were obtained (at magnification 40×) within the lesioned area, demarcated by FN staining, using the same settings for all image acquisition procedures. The red channel of the images, corresponding to PLP immunostaining, was then used for computer-assisted analysis. Non-specific labelling of objects other than myelin, such as artifactual spots resulting from tissue processing, was removed by despeckling, the contrast was increased and the threshold adjusted, using constant settings, before total object number was estimated by the software ($n = 6$/series for STX and AP groups and $n = 3$/series for the ungrafted group). The size and luminosity criteria used by the program for the definition of an object as a PLP$^+$ profile were kept constant in all measurements. Data on P0 and PLP are expressed per lesioned animal. Astrogliosis was estimated in the two grafted groups (STX and AP) using the Image-Pro Plus image analysis software by measuring GFAP immunoreactivity (in the red channel, as above) in the astrocyte dense area immediately adjacent to the FN$^+$ lesion site, in four sections spaced 80 µm apart for each animal, scanned at 10× ($n = 6$/series for STX and AP groups). Statistical analysis on the P0 data was performed using the Student's *t*-test, with $P < 0.05$ for significance. Statistical analysis on the PLP data was performed using one way ANOVA with $P < 0.05$ for significance, followed by Student's *t*-test between the groups.

To assess regeneration of 5-HT$^+$ fibres, sections double-labelled for 5-HT and FN (to demarcate the lesion site) were used and the fluorescence corresponding to 5-HT$^+$ staining was measured

using the Image-Pro Plus image analysis software, as follows. Three equal size strips (250 μm wide; total area 0.3125 mm^2), perpendicular to the rostrocaudal axis of the spinal cord and spanning the cord from the dorsal to ventral side, were scanned per section in four sections per animal (at magnification 40×) using the same settings for all image acquisition procedures. One strip was at 1-mm rostral to the edge of the lesion, one in the centre of the lesion and one immediately caudal to the edge of the lesion. Quantification of fluorescence was performed by image processing with the Image-Pro Plus image analysis software using the red channel of the images, corresponding to 5-HT^+ immunostaining. The results for the lesion site and caudal area were expressed as percentages of the fluorescence in the rostral area. Statistical analysis was performed using one way ANOVA with $P<0.05$ for significance.

Results

Expression of PSA-NCAM by STX-transduced GFP-SCs *in vitro*

Cultures of non-transduced SCs derived from embryonic or neonatal nerves do not express PSA (Lavdas *et al.*, 2006). However, when these cells are exposed to the pREV-STX retroviral vector, practically all become positive for PSA after selection with G418 (Lavdas *et al.*, 2006). Similarly, GFP-SCs were 100% positive for PSA after transduction with the pREV-STX retrovirus and selection (Fig. 1) while PSA could be effectively sheared off their surface with endoneuraminidase treatment (not shown). GFP-SCs exposed to pREV-AP were also 100% positive for AP but negative for PSA (not shown).

Integration of STX-transduced SCs within astrocyte territories *in vitro*

We have previously shown that STX-SCs grafted in cultured brain slices are better integrated in the complex CNS environment than non-transduced SCs (Lavdas *et al.*, 2006). As astrocytes are a major factor that hinders SC migration and integration in the CNS (Blakemore and Franklin, 2000; Iwashita *et al.*, 2000), we set out to examine directly the interaction of these two cell types *in vitro*. To address this, astrocytes (>95% positive for GFAP, data not shown) were plated as a strip of cells ~1 mm opposite a similar strip of either STX- or AP-GFP-SCs and were allowed to grow for 3 weeks (confrontation assay, Fig. 2A). As the cells within the two strips divided (mainly the astrocytes, data not shown) and migrated, they spread out and eventually came into contact. At the end of the 3 weeks, cultures were fixed and analysed. As identified by GFP fluorescence, expansion of the AP-GFP-SC population met an abrupt stop when it encountered the astrocytic domain, thus creating a distinctive boundary between the two cell populations (Fig. 2D and F). In contrast, STX-GFP-SCs entered readily the astrocyte area so that the two populations mixed (Fig. 2C and E). To quantify the ability of SCs to intermingle with astrocytes, the total number of GFP-SCs present in the astrocyte domain was counted in four cultures per condition. On average only 1.2 ± 0.2 AP-GFP-SCs/mm^2 were counted into the astrocyte territory while the average number of STX-GFP-SCs within the astrocytic region was 13.6 ± 0.8 cells/mm^2, which corresponds to an 11.3-fold increase ($P=0.0004$) (Fig. 2B).

Effects of STX-transduced GFP-SCs after transplantation in the mouse SCI model

Animals grafted with STX-GFP-SCs show improved hind limb locomotor function

Based on our current and previous (Lavdas *et al.*, 2006) *in vitro* results concerning the properties of STX-SCs we investigated their effect on functional recovery of mouse SCI. STX- and AP-GFP-SCs were transplanted in compression-lesioned mouse spinal cords and hind limb locomotor functional recovery was assessed using the BMS. Each group of animals was tested weekly up to 1 month after injury. The animals of the ungrafted group showed severe impairment of locomotor activity at all time points while the animals of the AP group showed some improvement at 4 weeks post-operation (Fig. 3). In sharp contrast, the animals of the STX group exhibited improved locomotor recovery as soon as the 2nd post-operative week, suggesting an early beneficial effect of the grafted STX-GFP-SCs. Hind limb locomotor performance was dramatically improved in the STX group at 3 weeks and remained high (and significantly greater than in the AP group) at 4 weeks post-operation (Fig. 3). One way ANOVA analysis showed a group effect with $P<0.05$, indicating significant overall differences between the different transplantation groups.

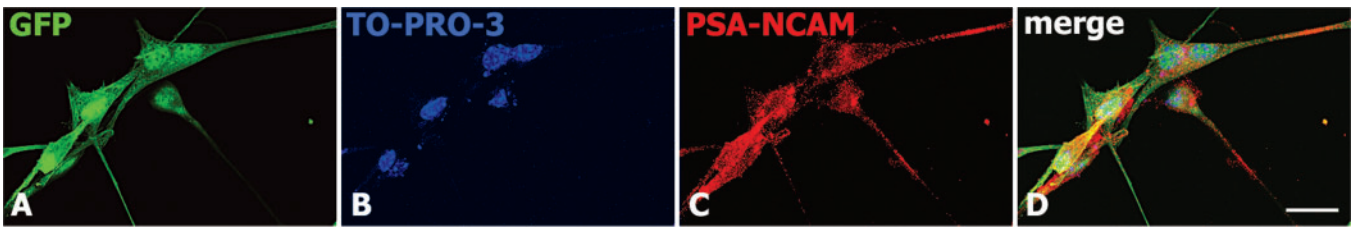

Fig. 1 STX-transduced SCs derived from transgenic actin-GFP mice after selection in G418 are all positive for PSA-NCAM. GFP fluorescence (green, **A**), oval-shaped SC nuclei labelled with TO-PRO-3 (blue, **B**), PSA-NCAM (red, **C**) and merged figure (**D**). Scale bar: 20 μm.

Migration and proliferation of transplanted GFP-SCs into the lesion site

After traumatic lesion of the spinal cord, a dense fibronectin-positive (FN^+) connective tissue matrix fills the lesion site, allowing a clear identification of the injury site (Camand *et al.*, 2004). This FN^+ area (Fig. 4A) is delimited by a $GFAP^+$ area (Fig. 4B). The $GFAP^+$ area with higher cellular density immediately adjacent to the FN^+ region is formed by reactive astrocytes and corresponds to the glial scar (Fawcett and Asher, 1999). After transplantation in the lesioned spinal cord, rostrally to the injury site, both STX- and AP-GFP-SCs migrated into and fully populated the FN^+ region of the lesion (Fig. 4C and D; see also Fig. 7). Estimation of GFAP immunoreactivity of the astrocytes within the glial scar region adjacent to the FN^+ area, 4 weeks after injury (Fig. 4), resulted in no apparent difference in the levels of astrogliosis between STX and AP-groups (data not shown).

The longest distance from the injection site at which GFP-SCs migrated caudally was measured under a fluorescence microscope using a graduated eyepiece grid and was found similar in both cases, 2 weeks after transplantation (STX-GFP-SCs: $2210 \pm 241\,\mu m$, AP-GFP-SCs: $2750 \pm 237\,\mu m$, $P = 0.145$). At 4 weeks practically all cells from both groups had populated the lesion site. Thus the two cell types were similarly distributed in the lesioned CNS, at 2 and 4 weeks after grafting, despite their different *in vitro* migratory behaviour (Lavdas *et al.*, 2006). This may be explained by the fact that, although STX-GFP-SCs were positive for PSA at the time of grafting, PSA expression was not detected on these cells 2 weeks after transplantation. In keeping with this down-regulation,

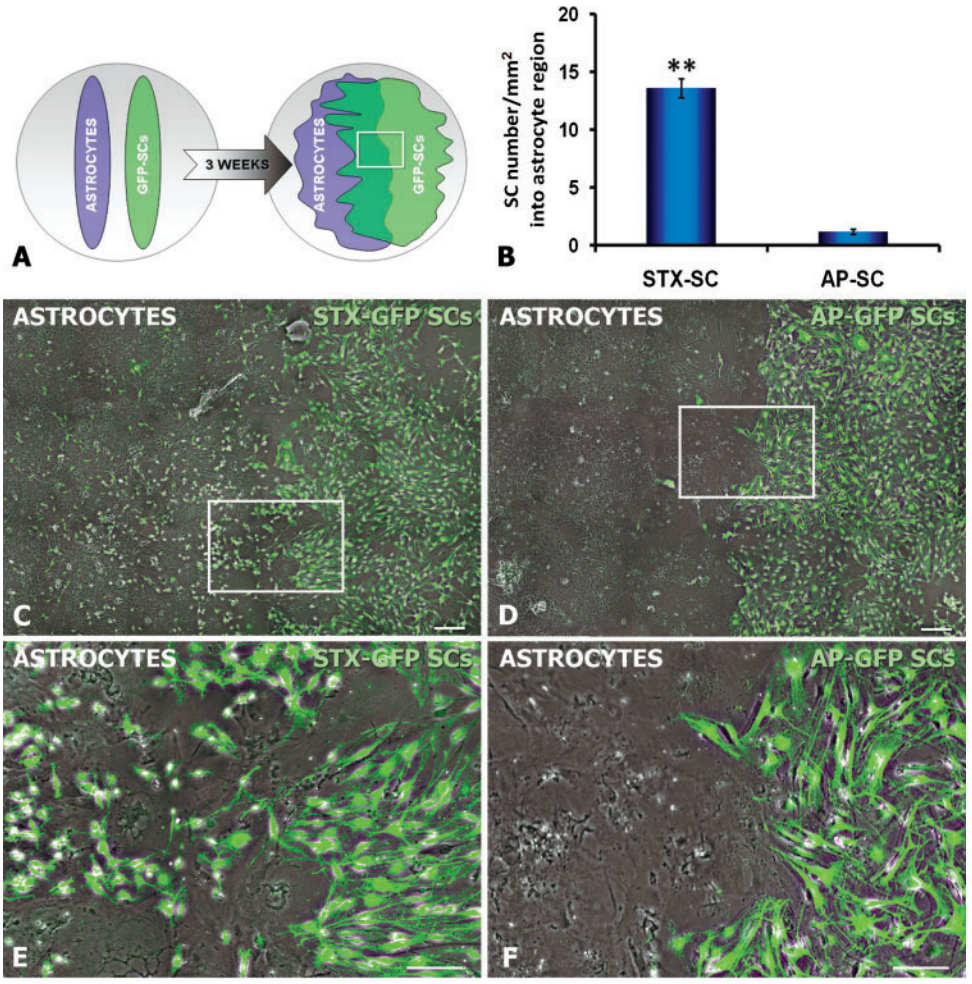

Fig. 2 Astrocyte-SC confrontation assay. (**A**) Astrocytes and GFP-SCs transduced with either STX or AP were plated in parallel strips as shown schematically in (**A**) and were allowed to grow and intermingle for 3 weeks. The inset in (**A**) refers to co-culture areas shown in (**C–F**). Astrocytes (phase contrast optics) were confronted with STX-GFP-SCs (green, **C**) or AP-GFP-SCs (green, **D**). Note the distinctive boundary formed when AP-GFP-SCs are confronted with astrocytes. In sharp contrast STX-GFP-SCs are able to penetrate the astrocyte boundaries and populate the astrocytic domain (**C**). (**E**, **F**) are higher magnifications of the rectangles marked in (**C**) and (**D**), respectively. Scale bars: (**C**, **D**), 200 μm; (**E**, **F**), 100 μm. (**B**) Quantification of the number of STX-GFP-SCs or AP-GFP-SCs found within the astrocytic territory ($n = 4$ in each case). **Student's *t*-test, $P < 0.01$. Error bars represent SEM.

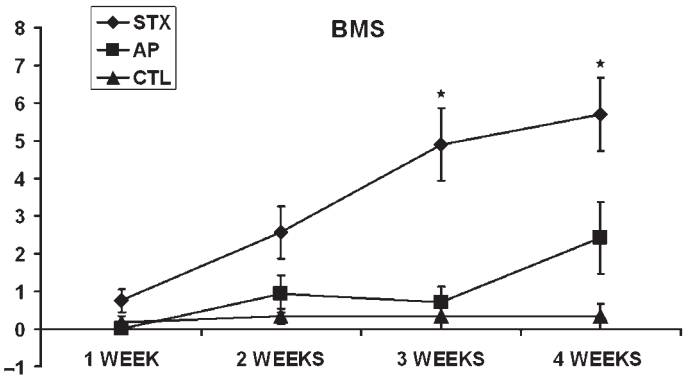

Fig. 3 Ability of STX-GFP-SCs to promote functional recovery after transplantation in the injured spinal cord. Recovery was assessed by using the BMS score, 1–4 weeks after grafting. The animals of the STX group show significant improvement of their hind limb locomotor skills from the second week after injury followed by dramatic improvement at 3 and 4 weeks, as compared to the AP group and to the ungrafted group (CTL). The animals of the AP group exhibit no difference when compared to the ungrafted group during the first 3 weeks and show improved motor performance of their hind limbs only at 4 weeks, though to a lesser extend than the STX group. The animals of the ungrafted group exhibit no recovery. *ANOVA, showed a group effect ($P < 0.05$), indicating significant overall differences between the different transplantation groups. Error bars represent SEM.

initial differences in the migration potential between the two groups of transplanted cells would be counterbalanced after 2 weeks *in vivo*.

In an attempt to define the time window of PSA expression by the grafted STX-GFP-SCs, we analysed an additional series of lesioned animals sacrificed at shorter time points, namely 1 day, 3 days, 1 week and 2 weeks after operation. PSA expression was detectable on the grafted STX-GFP-SCs at 1 (not shown) and 3 days (Fig. 5A) and to a lesser extent up to 1 week *in vivo* (not shown) while AP-GFP-SCs did not express PSA at any time-point tested (Fig. 5B).

Absence of PSA in STX-transduced SCs, 2 weeks after the lesion, may be due either to triggering of an endogenous differentiation program in the transplanted SCs (Lavdas *et al.*, 2006) or to vector silencing. As a means to distinguish between these two possibilities, we examined AP expression by NBT/BCIP histochemistry, in the transplanted AP-GFP-SCs of the AP group at 2 and 4 weeks after injury. We observed that AP-GFP-SCs did express alkaline phosphatase (Fig. 6), both at 2 and 4 weeks. Thus the AP transgene was expressed *in vivo* for at least 1 month after injury. Since the two transgenes were inserted in and expressed via the same viral vector, it is highly unlikely that PSA down-regulation is due to vector silencing.

To check the proliferation potential of the grafted cells, lesioned animals received BrdU during their survival time. No GFP-SCs were found to incorporate

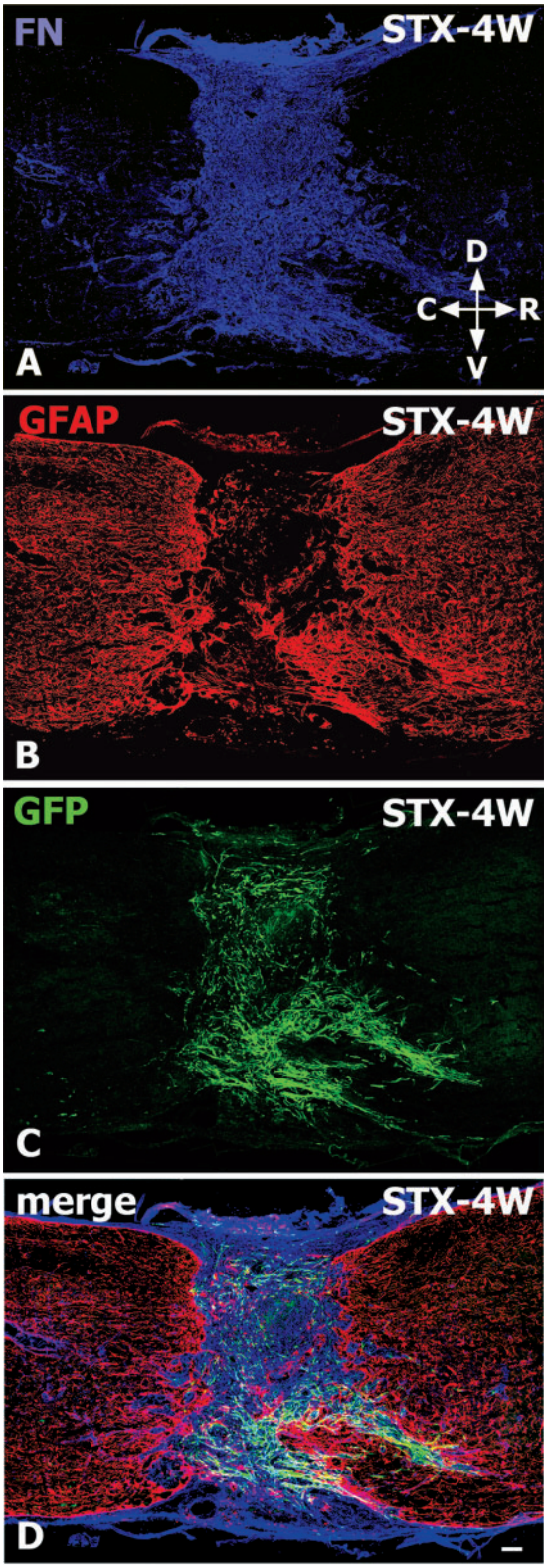

Fig. 4 Parasagittal section of the lesioned mouse spinal cord transplanted with STX-GFP-SCs, 4 weeks after injury. Double labelling for FN to illustrate the lesion site (blue, **A**) and GFAP immunoreactivity (red, **B**). Transplanted STX-GFP-SCs appear in green (**C**) and the merged picture is shown in (**D**). Orientation is shown in (**A**): R, rostral; C, caudal; D, dorsal; V, ventral. Scale bar: 100 μm.

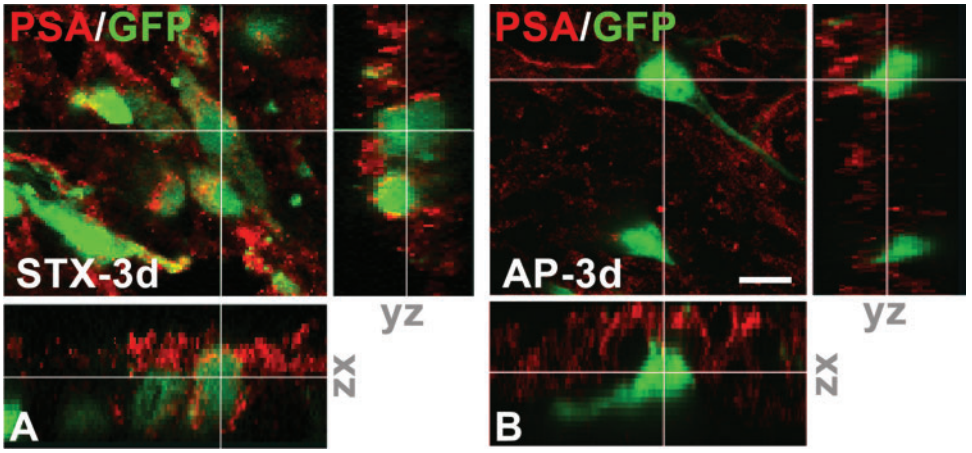

Fig. 5 Illustration of PSA expression by the grafted STX-GFP-SCs (**A**), in parasagittal sections of the injured mouse spinal cord, 3 days after transplantation. GFP-SCs appear in green and PSA immunolabelling in red. Colocalization is verified in the orthogonal projections. Grafted AP-GFP-SCs (**B**) were found negative for PSA at all time points checked (here at 3 days after injury). Micrographs represent single optical sections of confocal analysis. Scale bar: 10 μm.

BrdU either in the STX or in the AP group, 2 weeks (not shown) or 4 weeks after grafting (Fig. 7). Therefore transplanted STX-GFP-SCs do not proliferate, at least for the first 4 weeks after grafting, thus minimizing the possibility that these cells would become tumourigenic.

STX-transduced SCs promote sprouting of serotonergic axons into and across the lesion site

Given the fact that serotonergic (5-HT) fibres play important roles in locomotion (Barbeau and Rossignol, 1991) and in recovery after injury (Ribotta *et al.*, 2000), we examined whether 5-HT$^+$ axons enter the lesion site and cross its caudal border 2 and 4 weeks after operation in all the three groups of animals. To address this we performed double labelling for 5-HT and fibronectin to reveal the lesion site, combined with GFP detection of the grafted cells and confocal analysis (Fig. 8). We observed thin regenerating 5-HT$^+$ nerve fibres crossing the caudal border of the FN$^+$ region of the lesion site, in two out of six animals of the STX group (Fig. 8A and G) and in no animals of either the AP group or the ungrafted group, 2 weeks after transplantation (Fig. 8A–C). At 4 weeks, 5-HT$^+$ axons were observed to cross the caudal border of the lesion site in all six animals of the STX group (Fig. 8D and H), but only in three out of six animals of the AP group and in no animal of the ungrafted group (Fig. 8D–F; one-way ANOVA analysis showed a group effect with $P = 0.005$ at 4 weeks). Noticeably, closer observation at higher magnification revealed that the transplanted STX-GFP-SCs were in close proximity with the 5-HT$^+$ fibres within the FN$^+$ lesion site and the transduced SCs seemed to pave their way into and through the lesion site (Fig. 8I). Quantification of the effect at 4 weeks after injury, by computer-assisted estimation of 5-HT$^+$ fluorescence detected caudally to the lesion site, expressed as % of 5-HT$^+$ fluorescence detected rostrally to the lesion, revealed a statistically significant overall difference among the three experimental groups (one-way ANOVA, $P = 0.022$). Indeed, in the STX group there was a 13-fold increase in the value calculated as compared to the AP group (6.12 ± 2.09 versus $0.47 \pm 0.47\%$) while the value for the ungrafted group was zero (Fig. 8J). No statistically significant difference was found between groups for 5HT$^+$ fluorescence within the lesion site. These results suggest that the grafted STX-GFP-SCs render the CNS environment more permissive for axonal growth after SCI.

STX-transduced SCs remyelinate regenerating axons and promote remyelination by endogenous SCs

The potential of the grafted SC populations to remyelinate severed axons was evaluated by detection of GFP$^+$/P0$^+$ myelin internodes, 2 and 4 weeks after transplantation (Fig. 9). A fraction of either grafted cell type, STX- or AP-GFP-SCs, differentiated into myelin-forming cells though to a significantly different extent (Fig. 9). Thus remyelination by STX-GFP-SCs was 4.2-fold higher than remyelination by AP-GFP-SCs at 2 weeks ($P = 0.022$). As discussed earlier and consistent with the progression of these cells towards a differentiated promyelinating or myelinating state (Lavdas *et al.*, 2006), PSA expression was not detectable on STX-GFP-SCs by 2 weeks after injury. It has been reported that following SCI, endogenous SCs are recruited from the periphery to the lesion site through the dorsal root entry zones and contribute to remyelination (Beattie *et al.*, 1997; Brook *et al.*, 1998). Quantification of GFP$^-$/P0$^+$ myelin profiles revealed that the majority of P0-positive internodes encountered were GFP-negative (Fig. 9M), indicating that they originated from the host. Strikingly, remyelination by host SCs was enhanced by 11-fold in the STX group of animals as

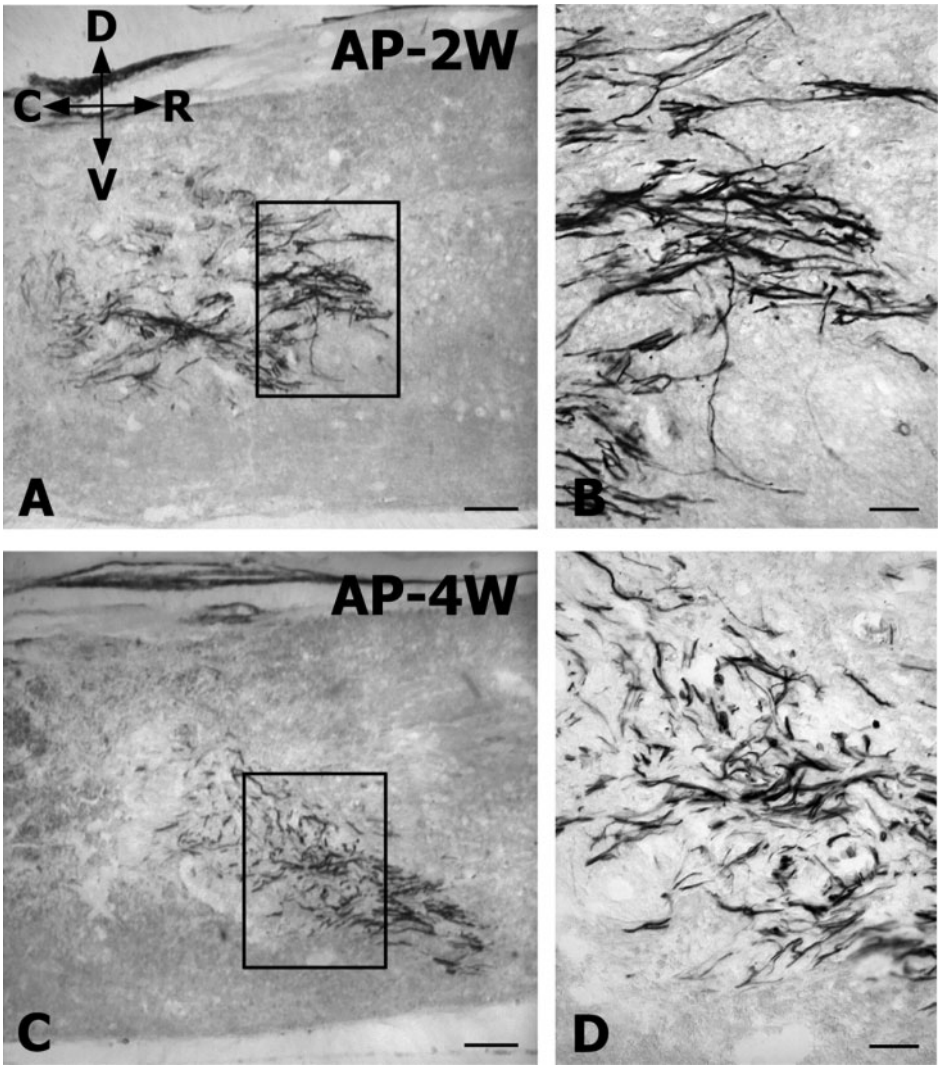

Fig. 6 Parasagittal sections of the lesioned spinal cord from animals of the AP group sacrificed at 2 (**A**, **B**) and 4 weeks (**C**, **D**). Alkaline phosphatase on the transplanted AP-GFP-SCs was visualised by histochemistry using NBT/BCIP as substrate and was detected both at 2 and 4 weeks after injury and SC transplantation. The insets in (**A**) and (**C**) are shown at higher magnification in (**B**) and (**C**), respectively. Orientation of sections is shown in (**A**); D, dorsal, R, rostral, V, ventral and C, caudal. Scale bar: (**A**, **C**), 150 μm; (**B**, **D**), 50 μm.

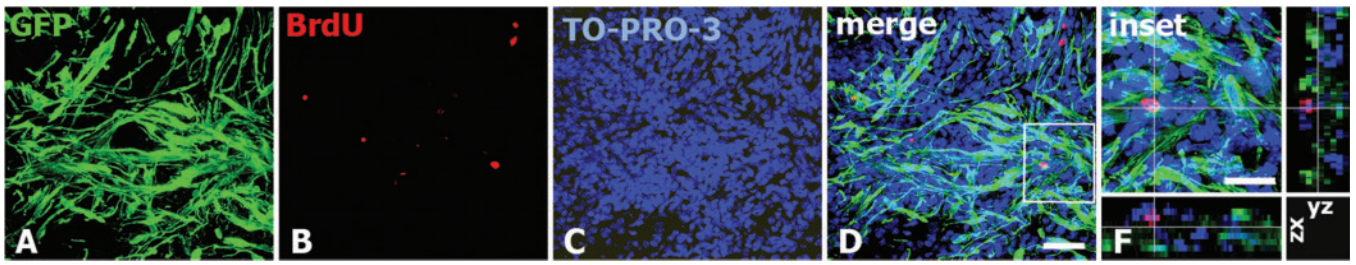

Fig. 7 Illustration of BrdU incorporation in a parasagittal section of the injured mouse spinal cord, 4 weeks after transplantation of STX-GFP-SCs. GFP-SCs appear in green (**A**), BrdU immunolabelling in red (**B**) and cell nuclei labelled with TO-PRO-3 in blue (**C**). As shown in the merged figure (**D**) and in the orthogonal projections (inset, **E**) there is no co-localization between BrdU and GFP, indicating that STX-GFP-SCs do not proliferate after transplantation. BrdU was administered in the drinking water of the lesioned animals until their sacrifice. Scale bars: 40 μm for (**A–D**), in (**D**); 20 μm in (**E**).

compared to the AP group ($P = 0.003$). Whereas all $GFP^+/P0^+$ internodes were restricted within the lesion site, $GFP^-/P0^+$ myelin internodes were observed both inside (Fig. 9A–H) and outside the lesion site (Fig. 9I–L). $GFP^-/P0^+$ myelin profiles were also detected in the ungrafted group and their numbers were not significantly different from those in the AP group ($P = 0.480$). Finally, we quantified the effect of the grafted cells to total

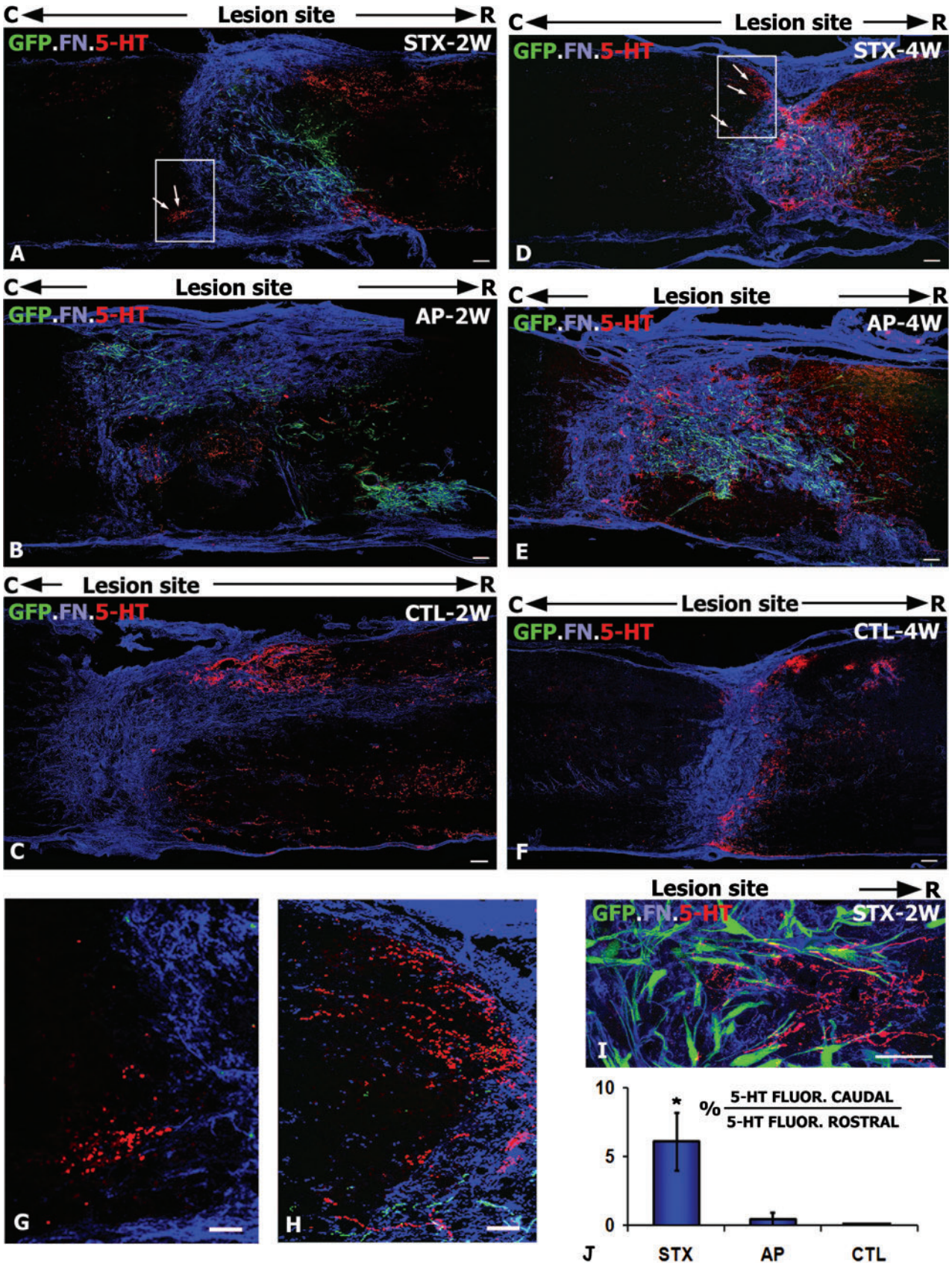

Fig. 8 Parasagittal sections of the lesioned mouse spinal cord, 2 weeks (**A–C**, **G** and **I**) and 4 weeks (**D–F** and **H**) after injury and grafting. Transplanted GFP-SCs, transduced with either STX or AP as indicated, appear in green, the lesion site is immunostained for FN (blue)

remyelination (by host and grafted SCs) based on the detection of all P0-positive profiles (Fig. 9M). Remyelination by both transplanted and host SCs in the STX group was 9.5-fold higher as compared to the AP group ($P = 0.003$). Again the difference between the AP group and the ungrafted group was not significant ($P = 0.408$).

At 4 weeks, the difference of the total remyelination index between the STX group and the AP group of mice is not significant ($P = 0.319$). However, there is still a significant difference in the remyelination held by host SCs, between the STX group and the ungrafted group (2.4-fold enhancement, $P = 0.013$) as well as between the AP group and the ungrafted group (2.2-fold enhancement, $P = 0.022$). In addition, total remyelination is 2.6-fold ($P = 0.012$) and 2.2-fold ($P = 0.023$) higher in the STX and the AP group, respectively, as compared to the ungrafted group (Fig. 9N). This is in agreement with previous findings showing that remyelination of regenerating axons is increased after SC transplantation in the demyelinated spinal cord (Baron-Van Evercooren *et al.*, 1991, 1992). Taken together, our results demonstrate that grafts of STX-GFP-SCs are capable of accelerating the process of remyelination. This is consistent with the improved locomotor activity manifested early on by the animals of the STX group. Even though total remyelination by SC eventually reaches similar levels after 4 weeks, in the STX and AP groups of mice, it seems that the earlier onset of remyelination observed in the STX group, probably contributes to the improved motor skills of these animals.

STX-GFP-SC grafts enhance remyelination by endogenous oligodendrocytes

The contribution of endogenous oligodendroglial precursors is crucial for remyelination after SCI. Presence of $NG2^+$ oligodendrocyte precursors was evident in all three groups of operated animals both within the lesion site (not shown) and surrounding area either rostral or caudal to the lesion, 3 days after injury (Fig. 10A and B). By 1 week after operation, numerous $NG2^+$ precursors were evident in the area surrounding the lesion only in the STX-group of animals while in both the AP and ungrafted groups a marked decrease in NG2-immunoreactive cells was evident (Fig. 10C and D). No differences in NG2-immunoreactivity were noted within the lesion site among the three groups. Thus, qualitatively, it appears that in the STX group there is prolonged recruitment of oligodendrocyte precursors in the area surrounding the lesion.

PLP is the major protein of central myelin (Anderson *et al.*, 1997). In order to evaluate the effect of the transplanted STX-GFP-SCs in the differentiation of oligodendroglial precursors to myelinating oligodendrocytes, we estimated by computer-assisted analysis the number of PLP^+ profiles within the lesion site of the two grafted groups (STX and AP) and of the ungrafted group of animals, 4 weeks after injury (Fig. 11). One-way ANOVA analysis showed a group effect with $P = 0.009$. A 2-fold increase of PLP^+ profiles was estimated in the STX group (Fig. 11A–C) as compared to the AP group (Fig. 11D–F) ($P = 0.0235$) and a 6.1-fold enhancement as compared to the ungrafted group ($P = 0.0038$). In addition, PLP^+ profiles were 3 times more abundant in the AP group than in the ungrafted group ($P = 0.0024$) (Fig. 11G). It is noteworthy that, qualitatively in the STX group of mice, a large number of PLP^+ profiles were found in areas populated by grafted STX-GFP-SCs (Fig. 11A–C). Thus although at 4 weeks the remyelination index of peripheral origin is similar in the STX and AP groups, there is significant difference in the remyelination index of central origin between the two groups. This is in agreement with the improved motor performances of the STX group of mice as estimated up to 4 weeks after grafting.

Discussion

Regulated expression of PSA has been shown to promote a reduction in cell–cell interactions that can create permissive conditions for architectural remodelling, an essential step towards CNS repair (Fujimoto *et al.*, 2001; Johnson *et al.*, 2005; El Maarouf *et al.*, 2006; Zhang *et al.*, 2007). In the present study, we have explored the potential of grafted STX-transduced SCs on the repair of the compression-lesioned mouse spinal cord. We have previously demonstrated that engineering SCs with a retroviral vector carrying the STX gene confers sustained PSA-NCAM expression on their cell surface (Lavdas *et al.*, 2006). STX-transduced SCs exhibit, in a short-term *in vitro* assay, enhanced motility in the CNS environment and, most important, retain their myelinating potential because of their ability to down-regulate PSA when primed to myelination. Here we have shown that when grafted in

and regenerating serotonergic fibres (5-HT^+) are shown in red. Thin regenerating 5-HT^+ fibres indicated by arrows in (**A**, **D**) are seen penetrating the spinal cord beyond the caudal border of the lesion site in the animals of the STX group, at 2 and 4 weeks after grafting. (**G**, **H**) are higher magnifications of the insets in (**A**) and (**D**), respectively. Numerous 5-HT^+ regenerating fibres are also discernible within the FN^+ lesion site of the STX group (**D**). In the animals of the AP group (**B**, **E**) a small number of 5-HT^+ fibres is observed in the FN^+ lesion site and, even fewer in the ungrafted CTL group (**C**, **F**) while there are no 5-HT^+ fibres in either of these groups close to or beyond the caudal border of the lesion site. (**I**) Reveals close association of STX-GFP-SCs and 5-HT^+ fibres within the FN^+ lesion site. R, rostral and C, caudal orientation. Dorsal is always at the top. Scale bars: (**A–F**), 100 μm; (**G–I**), 40 μm. (**J**) Quantification of 5-HT^+ fibre regeneration beyond the caudal edge of the lesion site 4 weeks after injury. The values were obtained as described in 'Materials and methods' section and represent the% ratio of fluorescence measured caudally to the lesion over the fluorescence measured rostrally to the lesion. *One-way ANOVA, $P < 0.05$. Error bars represent SEM.

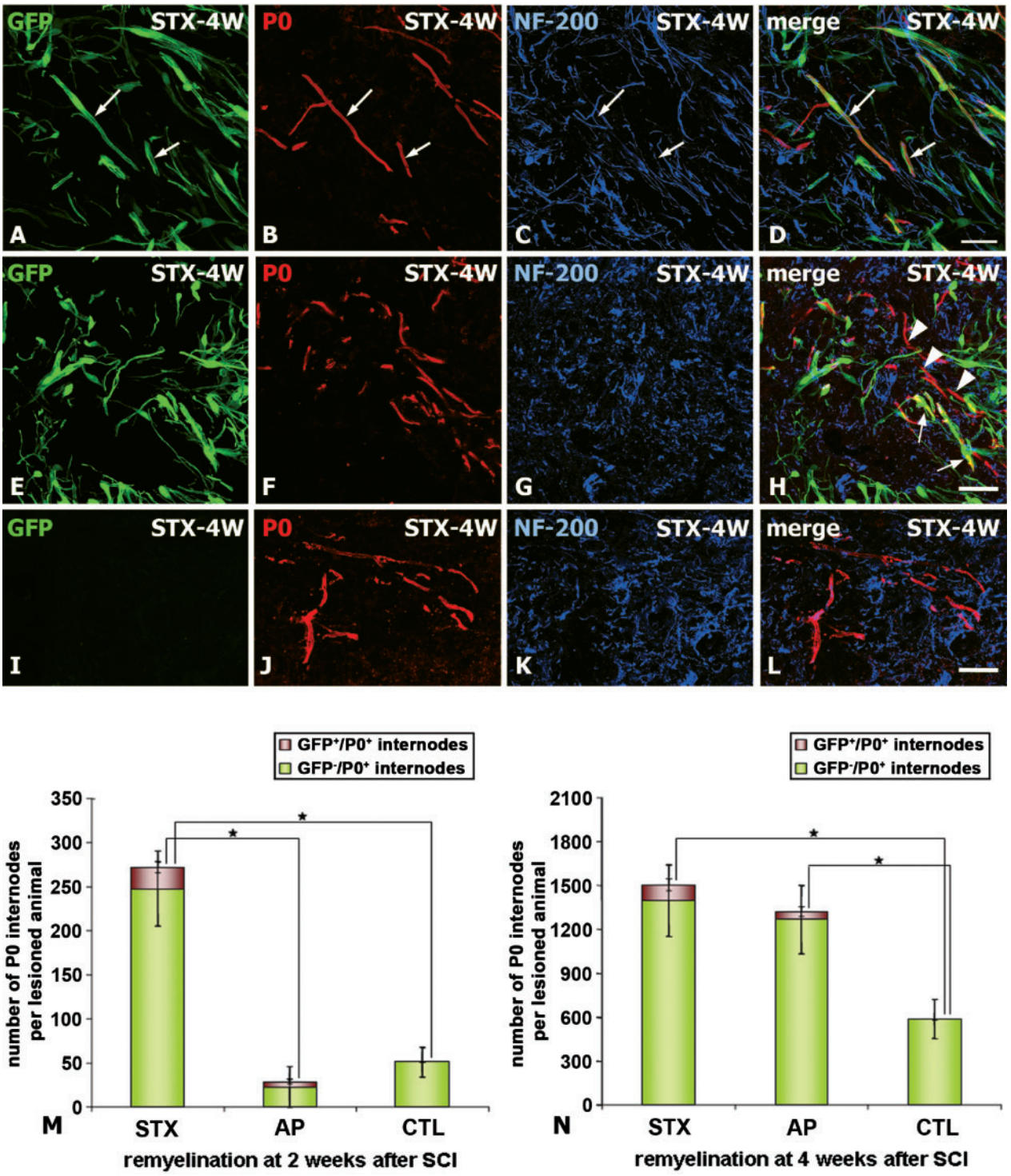

Fig. 9 Effect of STX-SC transplantation on remyelination by peripheral glia. (**A–L**) Double-immunofluorescence labelling of parasagittal sections of the lesioned spinal cord from an animal of the STX group, 4 weeks after injury. Areas inside (**A–H**) or outside (**I–L**) the lesion site are depicted. STX-GFP-SCs are shown in green (**A**, **E**), P0 myelin protein immunolabelling appears in red (**B**, **F**) and neurofilament (NF-200) immunolabelling in blue (**C**, **G**). The merged pictures are shown in (**D**, **H** and **L**). $GFP^+/P0^+$ internodes visible in (**D**) and (**H**) (arrows) are formed by transplanted STX-GFP-SCs while $GFP^-/P0^+$ internodes, mainly depicted in (**H**) (arrowheads) are formed by the host SCs. As illustrated in (**H**) and quantified in (**M**) the latter represent the majority of $P0^+$ internodes. Numerous $GFP^-/P0^+$ internodes are also detected outside the lesion area (L). Scale bar: 40 μm. (**M**, **N**) Quantification of remyelination by transplanted SCs ($GFP^+/P0^+$ internodes) and host SCs ($GFP^-/P0^+$ internodes), 2 and 4 weeks after injury. At 2 weeks (**M**) there is greatly enhanced remyelination by both transplanted and host SCs in the animals of the STX group as compared to the animals of the AP and the ungrafted (CTL) groups. At 4 weeks after injury (**N**) there is a significant difference between the remyelination in the two grafted groups as compared to the ungrafted (CTL) group, but not between the STX and the AP group. *Student's *t* test, $P < 0.05$. Error bars represent SEM.

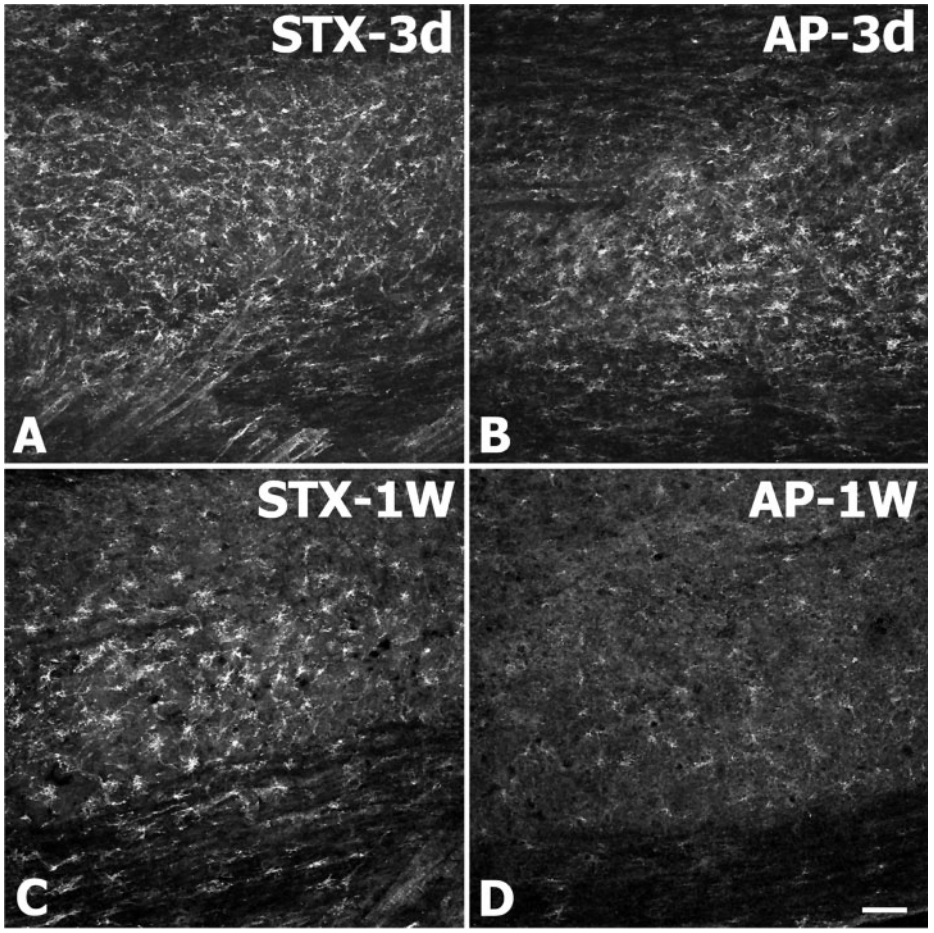

Fig. 10 Illustration of NG2 immunoreactivity on oligodendrocyte precursors, 2 mm rostrally to the lesion site. Three days after injury numerous NG2^{+} oligodendrocyte precursors are evident in animals of both the STX (**A**) and AP (**B**) groups. One week after injury, there is still high density of NG2^{+} cells in the STX group (**C**), while NG2 immunoreactivity is decreased in the AP group (**D**). Scale bar: 100 μm.

the injured spinal cord, STX-transduced SCs promoted functional recovery, which correlated with (a) enhanced remyelination rate both by grafted and host SCs and (b) enhanced differentiation/remyelination by resident oligodendrocyte precursors. In addition to enhancing remyelination, STX-SCs promoted sprouting of regenerating serotonergic nerve fibres into and beyond the lesion site. These results provide evidence that transplantation of genetically engineered SCs to express PSA-NCAM may be of therapeutic value for CNS myelin repair.

As astrocytes play a major role in the inhibition of SC migration and integration in the CNS (Blakemore and Franklin, 2000; Iwashita *et al.*, 2000), we first endeavoured to isolate this parameter and determine the biological consequences of PSA-NCAM expression by SCs on their ability to associate with astrocytes. When PSA-NCAM expressing SCs were confronted with astrocytes in culture, they showed a significantly improved integration within astrocytic territories as compared to control SCs transduced with a retroviral vector carrying the AP gene. This finding suggests that the reduced adhesion resulting from PSA expression (Fujimoto *et al.*, 2001; Johnson *et al.*, 2005) is enough to allow SCs to associate more effectively with astrocytes. However, despite their *in vitro* behaviour, the distribution of STX-transduced SCs was not significantly different from their control counterparts, at 2 and 4 weeks after grafting in the lesioned CNS. This may be explained by the fact that PSA appeared to decline already after 1 week *in vivo* and was no longer detectable on the grafted SCs at 2 weeks. This is a crucial observation with important consequences for the migration and myelination potential of the grafted SCs. One obvious constraint is that SC motility was not enhanced as much as originally anticipated, in the injured CNS. The early event of PSA down-regulation may also be responsible for the fact that STX-SCs were not detected caudally to the lesion site 4 weeks after grafting, despite their improved association with astrocytes *in vitro* (Lavdas *et al.*, 2006 and this study). However, we cannot preclude the action of other inhibitory cellular/molecular factors in the inhospitable environment of the lesioned CNS that are absent from purified astrocyte/SC co-cultures.

On the other hand, a most significant advantage of PSA down-regulation is that it allows early and enhanced

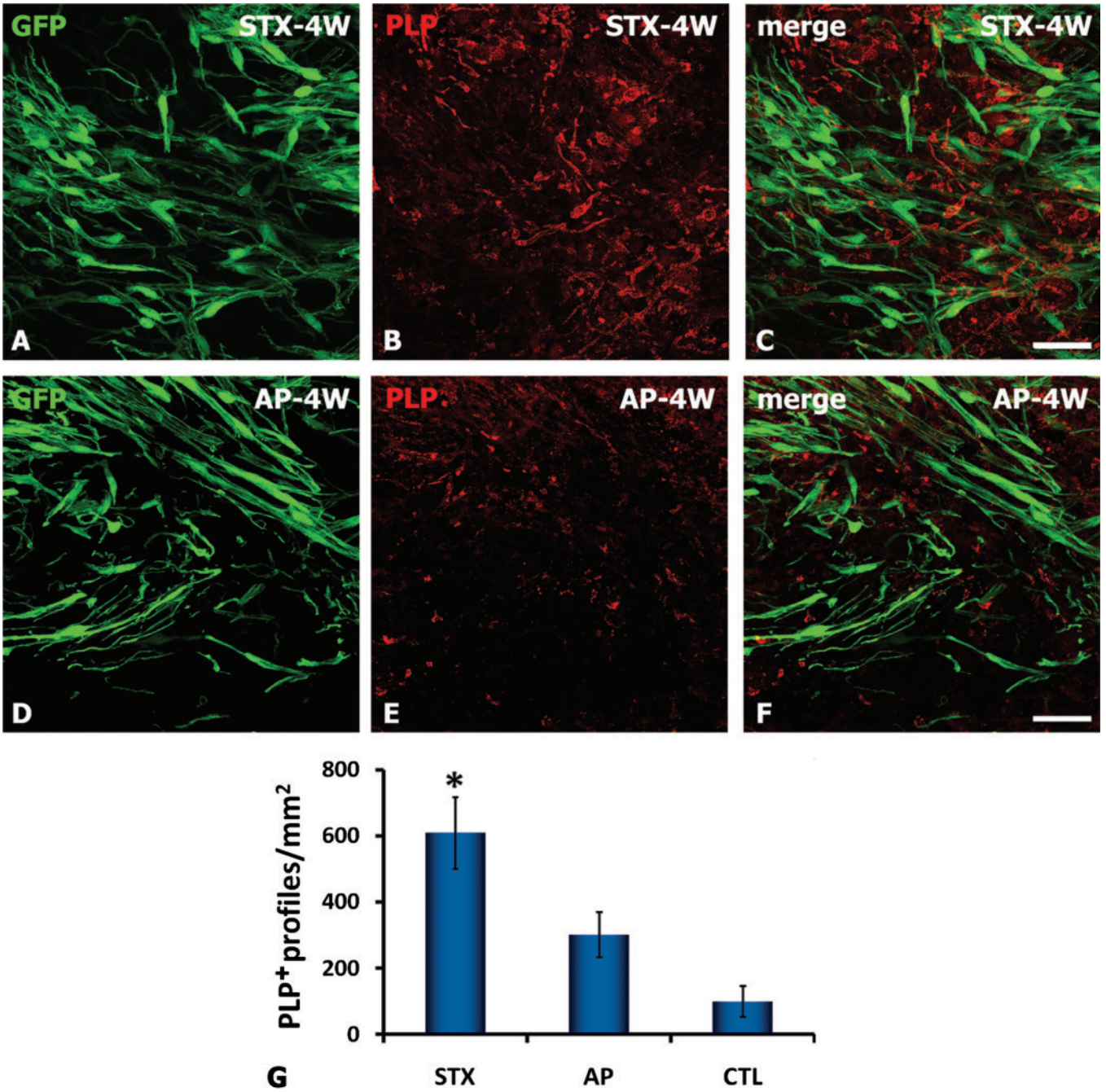

Fig. 11 Effect of STX-SC transplantation on remyelination by central glia. Parasagittal sections of the lesioned spinal cord from an animal of the STX group (**A–C**) or the AP group (**D**, **E**) at 4 weeks after injury. Grafted STX-GFP-SCs or AP-GFP-SCs appear in green (**A**, **D**) and PLP myelin protein in red (**B**, **E**). (**C**, **F**) are the merged pictures. A large number of PLP^+ profiles formed by oligodendrocytes are observed among the grafted SCs (**C**). Scale bar: 40 μm. (**G**) Quantification of remyelination of CNS origin (PLP^+ profiles) at 4 weeks after injury revealed significant enhancement of remyelination by oligodendrocytes in the animals of the STX group as compared to the animals of the AP and the ungrafted (CTL) group. *One-way ANOVA, $P < 0.05$. Error bars represent SEM.

myelination by the grafted SCs, which correlates with improved functional recovery. Since PSA acts as negative regulator of cell–cell interactions (Rutishauser, 1998; Charles *et al.*, 2000), maintaining PSA expression on myelin-forming cells could have instead hindered or, at best, delayed myelination with detrimental consequences for CNS repair. We maintain that, since AP was expressed by the grafted cells up to 4 weeks *in vivo*, it is highly unlikely that PSA down-regulation is due to silencing of the viral vector. Instead, it seems that PSA expression is regulated by environmental factors.

Previous studies have shown that SCs or peripheral nerve grafts in the CNS induce regeneration of axons, but neurites attempting to leave the SC environment of the

graft and re-enter the host CNS tissue fail to transverse the SC-astrocyte interface (Kao *et al.*, 1977; Xu *et al.*, 1997). Our results for serotonergic fibres are noteworthy, since $5HT^+$ fibres were observed growing caudally from the lesion site. It is not certain that all serotonergic fibres growing into and beyond the lesion site had regenerated from severed axons. Some fibres could be collateral sprouts from intact fibres spared after injury. It is clear, however, that STX-SCs facilitated the growth of these fibres that are important for locomotion (Barbeau and Rossignol, 1991) and recovery after injury (Ribotta *et al.*, 2000) and allowed them to surmount the inhibitory environment of the injured spinal cord.

An important finding is the observation that in the STX group of lesioned animals remyelination of severed axons was enhanced not only by grafted SCs but also by host SCs, most likely recruited from the periphery to the lesion site through the dorsal root entry zones (Beattie *et al.*, 1997; Brook *et al.*, 1998). Therefore it seems that grafted STX-SCs render the lesioned CNS more permissive to host SCs. It has been suggested that restriction of SC migration into astrocyte-rich regions may be mediated by contact inhibition, via *N*-cadherin (Wilby *et al.*, 1999; Fairless *et al.*, 2005). It is conceivable that the transient *in vivo* expression of PSA-NCAM on the surface of SCs reduces cadherin-mediated cell adhesion, thus enhancing SC integration in the damaged spinal cord. It is a noteworthy finding of the present study that PSA-NCAM expressing SCs seem to render the lesion site more permissive not only to host SCs but also to oligodendrocyte precursors that accumulate in the lesioned area and differentiate to mature myelinating oligodendrocytes. This was evident from the prolonged presence of $NG2^+$ precursors around the lesion. We speculate that during the period they express PSA-NCAM, STX-transduced SCs recruit, probably in a chain migration manner (Durbec and Cremer, 2001), SCs and oligodendrocyte precursors from the host that are also known to express PSA-NCAM for up to 2 weeks after demyelination (Oumesmar *et al.*, 1995). This major recruitment of myelinating glial cells both of peripheral and central origin results in higher rates of remyelination of the regenerating fibres. It is noteworthy that although at 4 weeks post-injury remyelination of peripheral origin is similar in the STX and AP groups, there is still significant difference in remyelination of central origin between the two groups. As a consequence the animals that received PSA-NCAM expressing SCs show significant improvement of their hind limb locomotor function as compared to control animals.

How do STX-SCs exert their beneficial action in SCI? Since PSA does not reduce astrogliosis (El Maarouf *et al.*, 2006 and this study), we hypothesize that the more permissive environment created by STX-SCs is due to an overall increased plasticity conferred by PSA expression, at least at the initial stages after SCI. PSA on NCAM can attenuate adhesion forces and modulate cell–surface interactions regulating cell movement in a non-specific manner (Rutishauser *et al.*, 1988). However, PSA may also be involved in specific signal transduction pathways triggered by growth factors. Thus PSA has been reported to modulate BDNF-, and FGF-dependent events such as cell survival, differentiation and synaptogenesis (Muller *et al.*, 2000; Vutskits *et al.*, 2001; Dityatev *et al.*, 2004). Moreover, PSA has been shown to influence p75 receptor activities (Gascon *et al.*, 2007) as well as NMDA receptor function (Bouzioukh *et al.*, 2001). Consequently, cellular responses to signalling events may be maintained even after PSA is down-regulated. Both of these non-exclusive modes of action, which entail non-specific modulation of cell adhesion and specifically triggered signal transduction mechanisms, may be operative in our study and their identification should point to potential alternative targets for clinical intervention.

To conclude, our results demonstrate in anatomical and behavioural terms, that transplantation of STX-SCs promotes the rate of remyelination, enhances axonal growth and improves locomotor function after SCI. The improvements in hind-limb performance are highly significant and, combined with the anatomical data, suggest that there is a critical time window for opportunity of repair after SCI. This proof of the concept that STX-SC grafts can foster a more permissive scar environment for remyelination/axonal growth may have important implications for therapeutic interventions to improve outcome after SCI. In particular, combinatorial approaches involving STX-SC grafts together with injection of PSA-mimicking peptides accelerating the migration of PSA-expressing cells (Torregrossa *et al.*, 2004; Florian *et al.*, 2006), may be of value for enhancing the spreading of STX-SCs in the spinal cord during the initial period that these cells are likely to express PSA.

Acknowledgements

We would like to thank Genevieve Rougon for generously providing antibodies to PSA; Monique Dubois-Dalcq and Anne Baron Van Evercooren for stimulating discussions and critical reading of the manuscript. This work was supported by the Wings for Life Spinal Cord Research Foundation grant WFL-FR-005/06 and GSRT EPAN Grants YB-11 and YB-26. Melitta Schachner is a New Jersey Professor of Spinal Cord Research.

References

Anderson TJ, Montague P, Nadon N, Nave KA, Griffiths IR. Modification of Schwann cell phenotype with Plp transgenes: evidence that the PLP and DM20 isoproteins are targeted to different cellular domains. J Neurosci Res 1997; 50: 13–22.

Angata K, Fukuda M. Polysialyltransferases: major players in polysialic acid synthesis on the neural cell adhesion molecule. Biochimie 2003; 85: 195–206.

Bachelin C, Lachapelle F, Girard C, Moissonnier P, Serguera-Lagache C, Mallet J, et al. Efficient myelin repair in the macaque spinal cord by autologous grafts of Schwann cells. Brain 2005; 128: 540–9.

Barbeau H, Rossignol S. Initiation and modulation of the locomotor pattern in the adult chronic spinal cat by noradrenergic, serotonergic and dopaminergic drugs. Brain Res 1991; 546: 250–60.

Baron-Van Evercooren A, Avellanna-Adalid V, Lachapelle F, Liblau R. Schwann cell transplantation and myelin repair of the CNS. Mult Scler 1997; 3: 157–61.

Baron-Van Evercooren A, Gansmuller A, Clerin E, Gumpel M. Hoechst 33342 a suitable fluorescent marker for Schwann cells after transplantation in the mouse spinal cord. Neurosci Lett 1991; 131: 241–4.

Baron-Van Evercooren A, Gansmuller A, Duhamel E, Pascal F, Gumpel M. Repair of a myelin lesion by Schwann cells transplanted in the adult mouse spinal cord. J Neuroimmunol 1992; 40: 235–42.

Beattie MS, Bresnahan JC, Komon J, Tovar CA, Van Meter M, Anderson DK, et al. Endogenous repair after spinal cord contusion injuries in the rat. Exp Neurol 1997; 148: 453–63.

Blakemore WF, Franklin RJ. Transplantation options for therapeutic central nervous system remyelination. Cell Transplant 2000; 9: 289–94.

Bouzioukh F, Tell F, Jean A, Rougon G. NMDA receptor and nitric oxide synthase activation regulate polysialylated neural cell adhesion molecule expression in adult brainstem synapses. J Neurosci 2001; 21: 4721–30.

Brook GA, Plate D, Franzen R, Martin D, Moonen G, Schoenen J, et al. Spontaneous longitudinally orientated axonal regeneration is associated with the Schwann cell framework within the lesion site following spinal cord compression injury of the rat. J Neurosci Res 1998; 53: 51–65.

Brustle O, Jones KN, Learish RD, Karram K, Choudhary K, Wiestler OD, et al. Embryonic stem cell-derived glial precursors: a source of myelinating transplants. Science 1999; 285: 754–6.

Bunge MB, Pearse DD. Transplantation strategies to promote repair of the injured spinal cord. J Rehabil Res Dev 2003; 40: 55–62.

Camand E, Morel MP, Faissner A, Sotelo C, Dusart I. Long-term changes in the molecular composition of the glial scar and progressive increase of serotoninergic fibre sprouting after hemisection of the mouse spinal cord. Eur J Neurosci 2004; 20: 1161–76.

Charles P, Hernandez MP, Stankoff B, Aigrot MS, Colin C, Rougon G, et al. Negative regulation of central nervous system myelination by polysialylated-neural cell adhesion molecule. Proc Natl Acad Sci USA 2000; 97: 7585–90.

Chen J, Bernreuther C, Dihne M, Schachner M. Cell adhesion molecule l1-transfected embryonic stem cells with enhanced survival support regrowth of corticospinal tract axons in mice after spinal cord injury. J Neurotrauma 2005; 22: 896–906.

Dityatev A, Dityateva G, Sytnyk V, Delling M, Toni N, Nikonenko I, et al. Polysialylated neural cell adhesion molecule promotes remodeling and formation of hippocampal synapses. J Neurosci 2004; 24: 9372–82.

Durbec P, Cremer H. Revisiting the function of PSA-NCAM in the nervous system. Mol Neurobiol 2001; 24: 53–64.

El Maarouf A, Petridis AK, Rutishauser U. Use of polysialic acid in repair of the central nervous system. Proc Natl Acad Sci USA 2006; 103: 16989–94.

Engesser-Cesar C, Anderson AJ, Basso DM, Edgerton VR, Cotman CW. Voluntary wheel running improves recovery from a moderate spinal cord injury. J Neurotrauma 2005; 22: 157–71.

Fairless R, Frame MC, Barnett SC. N-cadherin differentially determines Schwann cell and olfactory ensheathing cell adhesion and migration responses upon contact with astrocytes. Mol Cell Neurosci 2005; 28: 253–63.

Fawcett JW, Asher RA. The glial scar and central nervous system repair. Brain Res Bull 1999; 49: 377–91.

Florian C, Foltz J, Norreel JC, Rougon G, Roullet P. Post-training intrahippocampal injection of synthetic poly-alpha-2,8-sialic acid-neural cell adhesion molecule mimetic peptide improves spatial long-term performance in mice. Learn Mem 2006; 13: 335–41.

Fouad K, Schnell L, Bunge MB, Schwab ME, Liebscher T, Pearse DD. Combining Schwann cell bridges and olfactory-ensheathing glia grafts with chondroitinase promotes locomotor recovery after complete transection of the spinal cord. J Neurosci 2005; 25: 1169–78.

Franklin RJ. Remyelination of the demyelinated CNS: the case for and against transplantation of central, peripheral and olfactory glia. Brain Res Bull 2002; 57: 827–32.

Fujimoto I, Bruses JL, Rutishauser U. Regulation of cell adhesion by polysialic acid. Effects on cadherin, immunoglobulin cell adhesion molecule, and integrin function and independence from neural cell adhesion molecule binding or signaling activity. J Biol Chem 2001; 276: 31745–51.

Gascon E, Vutskits L, Jenny B, Durbec P, Kiss JZ. PSA-NCAM in postnatally generated immature neurons of the olfactory bulb: a crucial role in regulating p75 expression and cell survival. Development 2007; 134: 1181–90.

Girard C, Bemelmans AP, Dufour N, Mallet J, Bachelin C, Nait-Oumesmar B, et al. Grafts of brain-derived neurotrophic factor and neurotrophin 3-transduced primate Schwann cells lead to functional recovery of the demyelinated mouse spinal cord. J Neurosci 2005; 25: 7924–33.

Gravvanis AI, Lavdas A, Papalois AE, Franceschini I, Tsoutsos DA, Dubois-Dalcq M, et al. Effect of genetically modified Schwann cells with increased motility in end-to-side nerve grafting. Microsurgery 2005; 25: 423–32.

Halfpenny C, Benn T, Scolding N. Cell transplantation, myelin repair, and multiple sclerosis. Lancet Neurol 2002; 1: 31–40.

Honmou O, Felts PA, Waxman SG, Kocsis JD. Restoration of normal conduction properties in demyelinated spinal cord axons in the adult rat by transplantation of exogenous Schwann cells. J Neurosci 1996; 16: 3199–208.

Iwashita Y, Fawcett JW, Crang AJ, Franklin RJ, Blakemore WF. Schwann cells transplanted into normal and X-irradiated adult white matter do not migrate extensively and show poor long-term survival. Exp Neurol 2000; 164: 292–302.

Johnson CP, Fujimoto I, Rutishauser U, Leckband DE. Direct evidence that neural cell adhesion molecule (NCAM) polysialylation increases intermembrane repulsion and abrogates adhesion. J Biol Chem 2005; 280: 137–45.

Kao CC, Chang LW, Bloodworth JMJr.. Axonal regeneration across transected mammalian spinal cords: an electron microscopic study of delayed microsurgical nerve grafting. Exp Neurol 1977; 54: 591–615.

Kiss JZ, Rougon G. Cell biology of polysialic acid. Curr Opin Neurobiol 1997; 7: 640–6.

Lakatos A, Franklin RJ, Barnett SC. Olfactory ensheathing cells and Schwann cells differ in their in vitro interactions with astrocytes. Glia 2000; 32: 214–25.

Lavdas AA, Franceschini I, Dubois-Dalcq M, Matsas R. Schwann cells genetically engineered to express PSA show enhanced migratory potential without impairment of their myelinating ability in vitro. Glia 2006; 53: 868–78.

Levi AD, Bunge RP, Lofgren JA, Meima L, Hefti F, Nikolics K, et al. The influence of heregulins on human Schwann cell proliferation. J Neurosci 1995; 15: 1329–40.

McCarthy K, de Vellis J. Preparation of separate astroglial and oligodendroglial cell cultures from rat cerebral tissue. J Cell Biol 1980; 85: 890–902.

Meintanis S, Thomaidou D, Jessen KR, Mirsky R, Matsas R. The neuron-glia signal beta-neuregulin promotes Schwann cell motility via the MAPK pathway. Glia 2001; 34: 39–51.

Muller D, Djebbara-Hannas Z, Jourdain P, Vutskits L, Durbec P, Rougon G, et al. Brain-derived neurotrophic factor restores long-term potentiation in polysialic acid-neural cell adhesion molecule-deficient hippocampus. Proc Natl Acad Sci USA 2000; 97: 4315–20.

Oumesmar BN, Vignais L, Duhamel-Clerin E, Avellana-Adalid V, Rougon G, Baron-Van Evercooren A. Expression of the highly polysialylated neural cell adhesion molecule during postnatal myelination and following chemically induced demyelination of the adult mouse spinal cord. Eur J Neurosci 1995; 7: 480–91.

Pearse DD, Bunge MB. Designing cell- and gene-based regeneration strategies to repair the injured spinal cord. J Neurotrauma 2006; 23: 438–52.

Pearse DD, Marcillo AE, Oudega M, Lynch MP, Wood PM, Bunge MB. Transplantation of Schwann cells and olfactory ensheathing glia after spinal cord injury: does pretreatment with methylprednisolone and interleukin-10 enhance recovery? J Neurotrauma 2004; 21: 1223–39.

Pluchino S, Martino G. The therapeutic use of stem cells for myelin repair in autoimmune demyelinating disorders. J Neurol Sci 2005; 233: 117–9.

Ribotta MG, Provencher J, Feraboli-Lohnherr D, Rossignol S, Privat A, Orsal D. Activation of locomotion in adult chronic spinal rats is achieved by transplantation of embryonic raphe cells reinnervating a precise lumbar level. J Neurosci 2000; 20: 5144–52.

Rutishauser U. Polysialic acid at the cell surface: biophysics in service of cell interactions and tissue plasticity. J Cell Biochem 1998; 70: 304–12.

Rutishauser U, Acheson A, Hall AK, Mann DM, Sunshine J. The neural cell adhesion molecule (NCAM) as a regulator of cell-cell interactions. Science 1988; 240: 53–7.

Rutkowski JL, Kirk CJ, Lerner MA, Tennekoon GI. Purification and expansion of human Schwann cells in vitro. Nat Med 1995; 1: 80–3.

Storms SD, Rutishauser U. A role for polysialic acid in neural cell adhesion molecule heterophilic binding to proteoglycans. J Biol Chem 1998; 273: 27124–9.

Takami T, Oudega M, Bates ML, Wood PM, Kleitman N, Bunge MB. Schwann cell but not olfactory ensheathing glia transplants improve hindlimb locomotor performance in the moderately contused adult rat thoracic spinal cord. J Neurosci 2002; 22: 6670–81.

Thomaidou D, Coquillat D, Meintanis S, Noda M, Rougon G, Matsas R. Soluble forms of NCAM and F3 neuronal cell adhesion molecules promote Schwann cell migration: identification of protein tyrosine phosphatases zeta/beta as the putative F3 receptors on Schwann cells. J Neurochem 2001; 78: 767–78.

Thuret S, Moon LD, Gage FH. Therapeutic interventions after spinal cord injury. Nat Rev Neurosci 2006; 7: 628–43.

Torregrossa P, Buhl L, Bancila M, Durbec P, Schafer C, Schachner M, et al. Selection of poly-alpha 2,8-sialic acid mimotopes from a random phage peptide library and analysis of their bioactivity. J Biol Chem 2004; 279: 30707–14.

Vutskits L, Djebbara-Hannas Z, Zhang H, Paccaud JP, Durbec P, Rougon G, et al. PSA-NCAM modulates BDNF-dependent survival and differentiation of cortical neurons. Eur J Neurosci 2001; 13: 1391–402.

Wilby MJ, Muir EM, Fok-Seang J, Gour BJ, Blaschuk OW, Fawcett JW. N-Cadherin inhibits Schwann cell migration on astrocytes. Mol Cell Neurosci 1999; 14: 66–84.

Xu XM, Chen A, Guenard V, Kleitman N, Bunge MB. Bridging Schwann cell transplants promote axonal regeneration from both the rostral and caudal stumps of transected adult rat spinal cord. J Neurocytol 1997; 26: 1–16.

Zhang SC, Duncan ID. Remyelination and restoration of axonal function by glial cell transplantation. Prog Brain Res 2000; 127: 515–33.

Zhang Y, Ghadiri-Sani M, Zhang X, Richardson PM, Yeh J, Bo X. Induced expression of polysialic acid in the spinal cord promotes regeneration of sensory axons. Mol Cell Neurosci 2007; 35: 109–19.